Date 20/04/2020
Our reference WES-2019-59

Contact person Giovanni Migliaccio
E-mail giovanni.migliaccio.it@gmail.com

Subject **Author's response (minor revisions)**

University of Pisa
Department of Civil and Industrial Engineering

Address
Largo Lucio Lazzarino, 2, 56122, Pisa, Italy

Dear Editor,

The authors would like to express their gratitude for the comments we have received, which have helped us to further improve the quality of the paper. The objective of this document is to provide an overview of the minor revisions implemented in the current version of the paper. A paper-marked up version provides a direct comparison between the current version of the paper and its previous version.

Your sincerely,

Giovanni Migliaccio

Section(s): Response to Editor's comments (minor revisions)

Note-1: Author's response to Editor's comment follows the comment itself and is in blue.

Note-2: At the end of the section above, a paper marked-up version is added (it provides a direct comparison between the current revised paper and its previous version).

Response to Editor's comments (minor revisions)

Comments to the Author:

Nice job addressing the substantive comments from the reviewers. See detailed notes for additional considerations for improvement prior to publication.

- Some minor comments for final clean-up before publication:
  Line 31 – bridge components
  Line 32 – research
  Line 33 – need comma after paper

  Apart for some minor changes (e.g. for clean-up as suggested above), the present version of the paper includes modifications based on the comments received on "Section 2" and "Section 6", as detailed hereafter.

- Section 2

  The main paragraphs of section 2 have been modified. In particular, its first paragraph in the revised paper (lines 39-54) now includes further information and citations to reviews on blades aero-elastic modeling, along with references to fast aerodynamic approaches (such as BEM) and multi-objective optimization tasks (e.g. the integrated optimization of aerodynamics, structural performance and control system behavior). Then, the attention is dedicated to structural approaches for complex beam-like structures (to which modern blades belong), which is the focus of this paper (lines 55-73). More precisely, some of the main modeling approaches and investigators have been mentioned, along with literature reviews which summarize available theories and complicating effects (e.g. non-uniform cross-sections, initial twist, taper, swept), pointing out the need for further investigation on models for complex non-prismatic cases. Finally, guidelines considered in this work to develop a mathematical model for complex non-prismatic structures (undergoing large deflections, 3d cross-sectional warprings, etc) have been introduced (lines 74-80).

- Section 6

  Overall conclusion has been broadened and reorganized. In particular, after recalling the objective of the present work (lines 411-416), the advantages of the proposed modeling approach (with respect to 3D-FEM) for structural modeling of non-prismatic beam-like structures have been highlighted (e.g. lines 420-425), as well as the assumption of small warpings and strains considered in this paper and the limitation of the analyses to the terms of order ε (lines 426-428). Finally, the next steps of the present research have been anticipated, e.g. the extension of the theoretical model by including higher order terms (lines 429-431), along with suggestions for other future activities of practical interest (see also lines 431-434), e.g. comparison analyses with other structural models not based on 3D-FEM (with the aim of assessing the performance of different models for non-prismatic beam-like structures in terms of information each approach can provide, computational efficiency and results accuracy).

Beam-like models for the analyses of curved, twisted and tapered HAWT blades in large displacements

Giovanni Migliaccio[1], Giuseppe Ruta[2], Stefano Bennati[1], Riccardo Barsotti[1]

[1]Civil and Industrial Engineering, University of Pisa, Pisa, 56122, Italy
[2]Structural and Geotechnical Engineering, University "La Sapienza" of Roma, Roma, I-00184, Italy

Correspondence to: Giovanni Migliaccio (giovanni.migliaccio.it@gmail.com)

Abstract. ~~The continuous effort~~Continuous ongoing efforts to better predict the mechanical behaviour of complex beam-like structures~~ like~~, such as wind turbine blades~~ is strictly related~~, are motivated by the need to ~~requirements of~~improve their performance ~~improvement~~ and reduce the costs~~ reduction. But~~, However, new design approaches and the increasing flexibility of ~~those~~such structures make their aero-elastic modelling ever more challenging. For the structural part of this modelling, the best compromise between computational efficiency and accuracy can be obtained ~~by a schematization~~via schematizations based on suitable beam-like elements. This paper addresses the modelling of the mechanical behaviour of beam-like structures which are curved, twisted and tapered in their ~~reference~~ unstressed state~~,~~ and undergo large displacements, in- and out-of-plane cross-sectional warping and small strains. A suitable model for the problem at hand is proposed. Analytical and numerical results obtained by ~~applying the proposed modelling approach, as well as comparison with 3D FEM results, are illustrated~~its application are presented and compared with results from 3D-FEM analyses.

1 Introduction

~~In~~New methods are continuously being sought to improve the ~~process~~performance and efficiency of ~~improving~~ horizontal axis wind turbines (HAWT~~) performance new methods are continuously being sought for capturing more~~). Specifically, such improvements aim to increase their energy~~, developing~~ capture capacity, develop more reliable structures, and ~~lowering the cost of~~lower overall energy costs (Wiser~~,~~ 2016). Such goals can be achieved through the use of advanced materials, the optimization of the aerodynamic and structural behaviour of the blades, and the exploitation of load control techniques (see, for example, Ashwill 2010, Bottasso 2012, Stäblein 2017). ~~But~~However, new design strategies and the increasing flexibility of those structures make ~~the~~ modelling ~~of~~ their aero-elastic behaviour ever more challenging. For the structural part of this modelling, schematizing the blades through suitable beam-like elements ~~can be~~may represent the best compromise between computational efficiency and accuracy. ~~But modern~~Modern blades are however very complex beam-like structures. They ~~can~~may be curved, twisted and also tapered in their unstressed state. Even ~~not considering~~ignoring the complexities related to the materials and loading conditions, their shape alone is sufficient to make ~~the~~ mathematical description of their mechanical behaviour a very challenging task. This ~~paper~~work addresses the modelling of the mechanical behaviour of

structures of this kind, with a particular focus on their main geometrical characteristics, such as the twist and taper of ~~their~~the transversal cross-sections, as well as the in- and out-of-plane cross-sectional warping ~~of their cross sections,~~ and the large deflections of their reference centre-line.

Over the years several theories have been developed for beam-like structures (see, for example, Love 1944, Antmann 1966, ~~and~~ Rubin 1997~~). This is because beam models have historically been used~~), for applications in ~~many~~different fields, from helicopter rotor blades in aerospace engineering to ~~bridges~~bridge components in civil engineering and surgical tools in medicine. Nevertheless, ~~the~~due to the continuous need for ever more rigorous and application-oriented models, interest in advanced theories for complex beam-like structures has led to further ~~researches also~~research even in recent years~~, due to the continuous need of ever more rigorous and application oriented models. In~~. The focus of this paper ~~the attention is focused~~is on the effects of important geometrical characteristics of those structures, such as the curvature of their centre-line, as well as the twist and the taper of their cross-sections. After an introduction to modelling approaches for structures of this kind (section 2), a suitable model is proposed for the problem at hand ~~is proposed~~ (section 3). Finally, analytical results and numerical examples obtained by applying the proposed modelling approach to reference beam-like structures are ~~illustrated~~presented and compared with results from 3D-FEM analyses (sections 4 and 5).

2 Overview of modelling approaches

~~Aero-elastic modelling of~~ Modelling the mechanical behaviour of modern blades can be ~~addressed by means of~~ performed via different approaches ~~(~~. See, for example, the reviews on aero-elastic modelling approaches for wind turbine blades of Hansen 2006 and Wang 2016a~~). Those ones~~, which discuss and compare aerodynamic and structural models used in research and industrial applications. For the structural modelling, two main choices are based on 3D FEM and beam models ~~are two main choices for the structural part of this modelling. Although~~. In general, 3D FEM approaches can be very accurate and flexible, but they can be computationally ~~expensive~~demanding for ~~the~~ analyses of complex systems, especially if they are coupled with CFD methods for aerodynamic analyses ~~are executed in parallel~~. The overall computational cost can be reduced ~~if~~using faster aerodynamic models ~~are used~~, such as those based on the blade element momentum ~~(BEM) model, but even this solution~~ theory (see, for example, Hansen 2006). However, this may not ~~be efficient enough for aero-elastic analyses and~~ yet be sufficient in the case of multi-objective optimization tasks~~. The coupling of BEM and~~, in which the optimization of several aspects (e.g. aerodynamic performance, structural characteristics and control systems) have to be addressed at the same time (see also Bottasso 2012). Therefore, faster structural models may be needed as well, such as suitable beam models ~~can be~~, which may provide accurate information on the deflection of the structure's centre-line, as well as the strain and stress fields in the three-dimensional solid. The use of fast aerodynamic models along with suitable beam models may then represent the best compromise between computational efficiency and accuracy. In this work ~~we~~, the focus ~~the attention on~~ is only on the structural modelling. In particular, a mathematical ~~models~~model is proposed to simulate the ~~mechanical~~ behaviour of ~~complex~~ non-prismatic beam-like structures ~~(hereafter referred to as beam-like models, or~~

BLM), which can, which may be curved, twisted and also tapered in their unstressed reference state, undergo large deflections, in- and out-of-plane cross-sectional warping and small strain. Suitable models are needed (such a model is referred to simulatehere as beam-like model or BLM).

Over the behaviour of thoseyears many approach have been developed for beam-like structures. In general, , from classical beam models (see, for example, Love 1944), which include for extension, twisttwisting and bending, as well as the to Reissner's formulation (1981), which also accountingaccounts for transverse shear deformation, may not be sufficient. Geometrically exact models are a better choice, but a way to put them into a suitable form for engineering applications is usually needed (Antman 1966). In general, suitable models should be both rigorous and application oriented, two important requirements pursued over the years by to geometrically exact and asymptotic approaches, involving the research efforts of many investigators (e.g.such as Antman 1966, Giavotto 1983, Simo 1985, Ibrahimbegovic 1995, Ruta 2006, Pai 2011, and Yu 2012).

For over a century researchers have sought to represent beam-like structures by means of 1D models. Several, Hodges 2018). The available theories have been developed, from the elementary Euler Bernoulli theory, to the classical theory which includes Saint-Venant torsion, up to more refined theories, such as the Timoshenko theory for transverse shear deformations, the Vlasov theory for torsional warping restraint, and 3D beam theories which include 3D warping fields. Broadly speaking, beam theories can bemay be broadly grouped into engineering theories and mathematical theories. Several engineering theories are ones. The former are usually based on ad-hoc corrections to simpler theories (e.g. Rosen 1978), others are based on) or exploit geometrically exact approaches (such as Wang 2016b and Hodges 2018). Among), the mathematical theories, some approacheslatter are generally based on the directed continuum (see, for example, Rubin 2000), some others) or exploit asymptotic methods (e.g. Yu 2012). The reason for such a large amount of worksReviews on beam theory is that it has always found applicationtheories are also available in many fields. By way of the literature, which summarize modelling approaches and complicating effects. For example, many approachestheories have been developed for helicopter rotor blades with an initial twist, but (Hodges 1990). In this regards, a wide-ranging review on pre-twisted rods have always attracted the interest of many researchers in several fields (is due to Rosen (1991). In the 1990's,), which covers several aspects of the problem, from the response to static loads, to dynamics and stability issues. Kunz (1994) also provided an overview on modelling methods for rotating beams, illustrating discussing how engineering theories for rotor blades evolved over the years. In those same years, Hodges (1990) reviewed the modelling approaches for composite rotor blades, discussing , from the recognition of the importance of 3D warping and deformation coupling.bending flexibility, to the development of linear equations for bending and torsion, to the introduction of nonlinear terms to such equations. More recently, Rafiee (2017) discussedreviewed the vibrations control issues in rotating beams, summarizing beam theories and complicating effects, such as non-uniform cross-sections, initial curvaturescurvature, twist and sweep. It In general, it seems that, unlike the case of the pre-twisted rods, the results published results for curved rotating beams with initial taper and sweep are quite scarce, although all these geometrical characteristics canmay play an important role. This is particularly true for modern wind

turbine blades, which are ever more flexible and longer than the past, pre-bent and swept and, in addition, are characterized by significant chord and twist variations.

~~Up to now much has~~ To date many research efforts have been ~~done~~devoted to ~~develop~~developing powerful ~~beam theories. However, there is still a gap between existing theories and those that could be suitable for complex~~theories for beam-like structures. However, complex non-prismatic cases still require further investigation. In general, the geometry of the reference and current states of the structure must be appropriately described~~. The~~, as the curvature, twist and taper are important geometrical design features and should be explicitly included in the model. ~~The~~Moreover, the analysis should not be restricted to small displacements. The model should provide the stress and strain ~~and stress~~ fields in the three-dimensional ~~beam like structure~~solid, be rigorous and ~~usable by engineers~~application-oriented, and provide classical results when applied to prismatic ~~isotropic homogeneous beams.~~cases. Following these guidelines, a mathematical model to simulate the mechanical behaviour of the ~~considered~~mentioned non-prismatic beam-like structures is proposed hereafter.

3 Mechanical model for complex beam-like structures

Here we are concerned with developing a mathematical model to describe the mechanical behaviour of beam-like structures which are curved, twisted and tapered in their reference state and undergo large displacements. One of the main issues with such a task is how to describe the motion of the structure ~~(see, for example,~~. See, among others, the works of Simo 1985, Ruta 2006~~,~~ and Pai 2014~~). The approach considered in this work is to imagine a~~ for some examples of different approaches. Here, we consider a non-prismatic beam-like structure as a collection of deformable plane figures (i.e. the reference cross-sections) along a ~~regular and simple~~suitable three-dimensional curve (i.e. the reference centre-line). We assume that each point of each cross-section in the reference state moves to ~~a~~its position in the current state through a global rigid motion on which a local general (warping) motion is superimposed. In this manner, the cross-sectional deformation can be examined independently of the global motion of the centre-line. ~~So, it~~It is thus possible to consider the global motion to be large, while the local motion and the strain may be small. An analytical description of how the motion of the considered structure is modelled in this work is presented and further discussed in the following section.

3.1 Kinematics and strain measures

We begin by introducing two local triads of orthogonal unit vectors. The first ~~one~~ is the local triad, b_i, in the reference state, with b_1 aligned to the tangent vector of the reference centre-line. This frame is a function of the reference arch-length s, that is $b_i=b_i(s)$. The second local triad, a_i, is a suitable image of the local triad b_i in the current state. This frame is a function of the reference arch-length s and ~~the~~ time t, that is $a_i=a_i(s,t)$. In general, a_1 is not required to be aligned to the tangent vector of the current centre-line. ~~See~~ Figure 1~~. It~~ shows a schematic representation of the reference (left) and current (right) states of a beam-like structure. The generic cross-section in the reference state is contained in the plane of ~~the~~ vectors b_2 and b_3. In the current state, if the cross-section remains plane (i.e. un-warped), it can belong to the plane of ~~the~~ vectors a_2 and a_3.

~~But~~However, the generic cross-section may not remain plane~~. So,~~, so we consider that its current (warped) state is ~~reached~~attained by superimposing an additional motion to the positions of the points of the un-warped cross-section, as in Figure 1 (right).

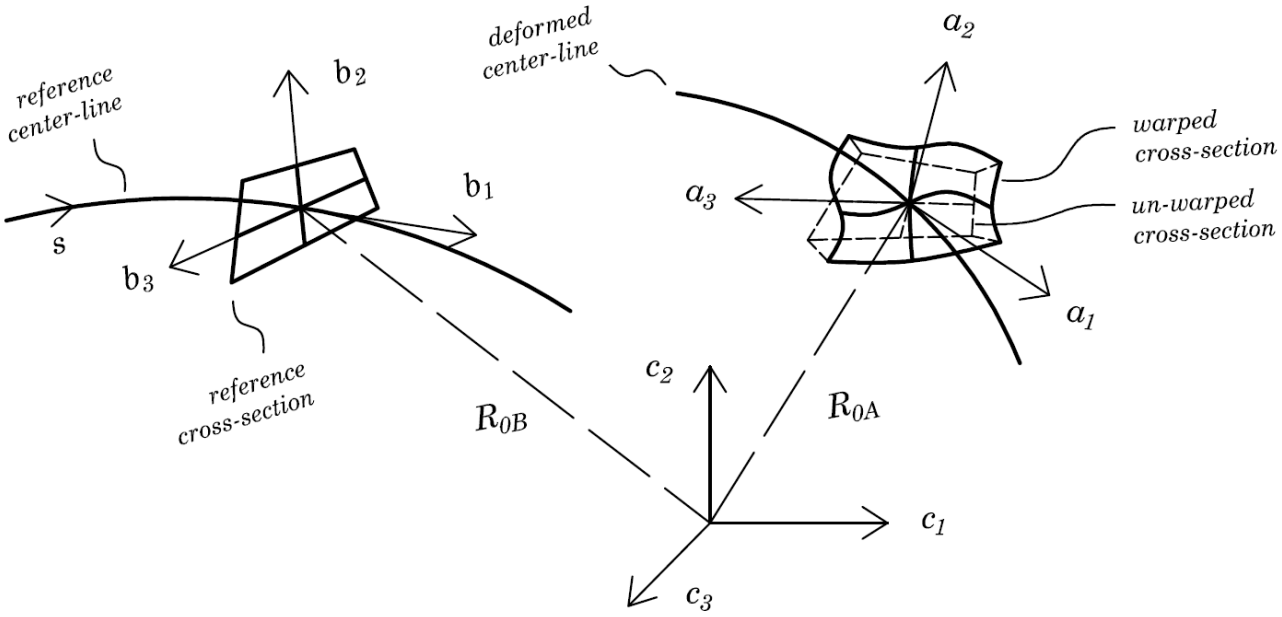

Figure 1: Schematic of the reference and current states, centre-lines, cross-sections and local frames

We continue by introducing the ~~kinematical~~kinematic variables we use to describe the motion of the considered structure. To this ~~aim~~end, the orientation of ~~the~~ frames a_i and b_i relative to a fixed rectangular frame, c_i, are defined as follows

$$a_i = Ac_i, \quad b_i = Bc_i \tag{1}$$

where A and B are two proper orthogonal tensor fields (i.e. their determinant is 1, see, for example, Gurtin 2003). We also introduce a tensor field, T, which defines the relative orientation between ~~the~~ frames a_i and b_i as follows

$$a_i = Tb_i = AB^T b_i \tag{2}$$

We define two skew tensor fields, K_A and K_B, and their axial vectors, k_A and k_B, which are related to the curvatures of the structure's centre-line ~~of the structure~~ in the current and reference states, as follows (see, for example, Simo 1985 and Gurtin 2003)

$$\begin{aligned} K_A &= A'A^T, \quad a_i' = K_A a_i = k_A \wedge a_i \\ K_B &= B'B^T, \quad b_i' = K_B b_i = k_B \wedge b_i \end{aligned} \tag{3}$$

where the prime denotes derivative with respect to the arch-length, s, while the operator $\wedge$ is the usual cross-product.

In a similar manner, we introduce the skew tensor field Ω, and its axial vector field ω, related to the variation of ~~the~~ vectors a_i over the time, t, as follows

$$\Omega = \dot{A}A^T, \quad \dot{a}_i = \Omega a_i = \omega \wedge a_i \tag{4}$$

The dot (over the variables) denotes derivative over the time, t. At this point, it is easy to obtain the following identities

$$\begin{aligned} T'T^T &= K_A - TK_BT^T, \quad \dot{T}T^T = \Omega \\ \phi\left[T'T^T\right] &= k_A - Tk_B, \quad \phi\left[\dot{T}T^T\right] = \omega \end{aligned} \tag{5}$$

where the operator ϕ[] provides the axial vector of the skew tensor between brackets.

~~The function~~Function R_{0B}, which maps the points of the centre-line in the reference state, does not depend on time, while R_{0A} can change over ~~the~~ time t. Its variation is the time rate of change of the position of the points of the current centre-line

$$\dot{R}_{0A} = v_0 \tag{6}$$

We are now in a position to introduce two important kinematic identities

$$\begin{aligned} v_0' - \omega \wedge R_{0A}' &= T\dot{\gamma} \\ \omega' &= T\dot{k} \end{aligned} \tag{7}$$

where γ and k are

$$\begin{aligned} \gamma &= T^T R_{0A}' - R_{0B}' \\ k &= T^T k_A - k_B \end{aligned} \tag{8}$$

It is worth ~~nothing~~noting that γ and k vanish for rigid motions and are invariant under superposed rigid motion, hence, they are well-defined measures of strain for beam-like structures (see, for example, Ruta 2006 and Rubin 2000).

Now, we start modelling the motion of the ~~points of the~~ cross-sections points. In particular, we introduce two mapping functions, R_A and R_B, to identify the positions of the points of the 3D beam-like structure in its current and reference states. ~~For what~~Regarding the reference state ~~is concerned~~, we define the (reference) mapping function

$$R_B(z_i) = R_{0B}(z_1) + x_\alpha(z_i) b_\alpha(z_1) \tag{9}$$

where R_{0B} is the position of the points of the reference centre-line relative to ~~the~~ frame c_i, b_α are the vectors of the reference local frame in the plane of the reference cross-section, x_α identify the ~~position~~positions of the points in the reference cross-section relative to the reference centre-line, and, finally, z_i are independent mathematical variables which ~~do not depend on~~are independent of time. In particular, z_1 is equal to the arch-length s, and z_α belong to a bi-dimensional mathematical domain which is used to map the position of the ~~points, x_α, of the~~ cross-sections points, x_α. Throughout this paper, Greek indices ~~assume~~take on values 2 and 3, Latin indices assumes values 1, 2 and 3, and repeated indices are summed over their range.

It is worth noting that x_k may or may not be equal to z_k. The ~~first choice~~former (equality) leads to ~~the most~~ common modelling approaches available in the literature (see, for example, Simo 1985, Pai 2011, and Yu 2012). ~~In this work~~Herein,

we choose a set of relations between the position variables x_k and the mathematical variables z_k to provide a description of the shape of the considered beam-like structure, which can be curved, twisted and also tapered in its reference state. In particular, the span-wise variation of the ~~shape of the~~ cross-sections shape is analytically modelled by means of a mapping of ~~this kind~~the following type

$$x_i = \Lambda_{ij} z_j \tag{10}$$

where the coefficients Λ_{ij} are functions of z_1. In the following, we will consider the case of the curved and twisted beam-like structures with bi-tapered cross-sections, in which case ~~the~~ map (10) reduces to

$$x_1 = z_1, \quad x_2 = z_2 \lambda_2(z_1), \quad x_3 = z_3 \lambda_3(z_1) \tag{11}$$

where ~~the~~ coefficients λ_α are functions of z_1. It is worth noting that a suitable choice of ~~those~~such functions ~~gives the possibility to reproduce~~enables reproducing interesting shapes. ~~See~~Figure 2, for example, ~~Figure 2. It~~ shows a 3D beam-like structure whose centre-line is curved, while the cross-sections are twisted and tapered from the root to the tip. The reference cross-sections in Figure 2 are ellipses with different sizes and orientations, but any other reference cross-section shape can be considered, such as the aerodynamic profiles which are commonly used for wind turbine blades, steam turbines blades, and helicopter rotor blades as well (see also Griffith 2011, Bak 2013, Tanuma 2017, and Leishmain 2006 for examples of such profiles).

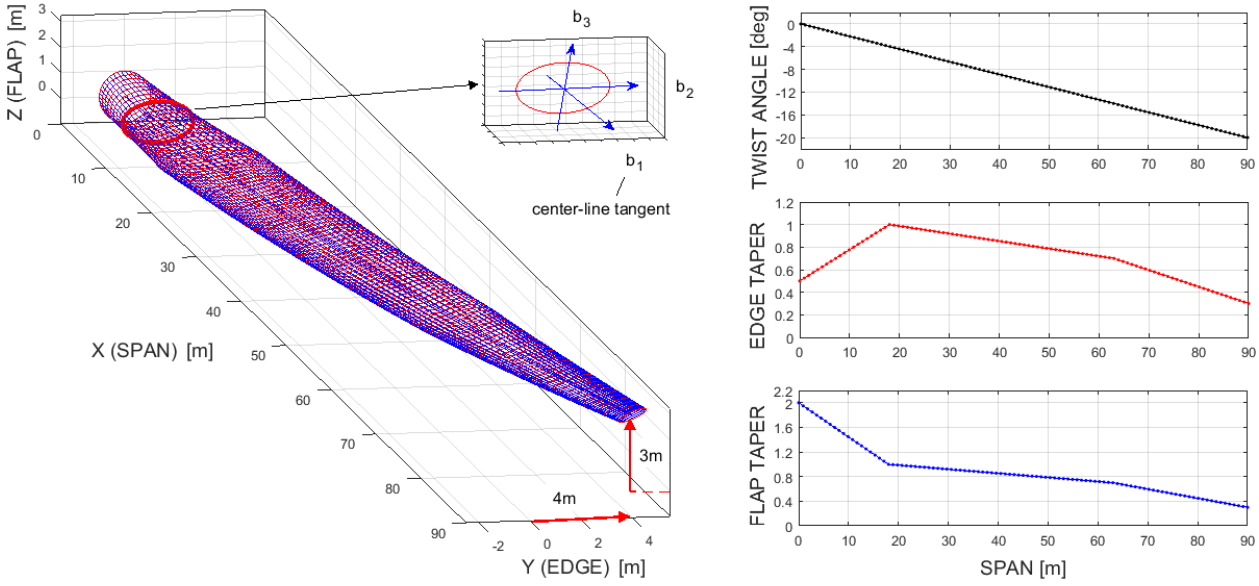

Figure 2: Example ~~of~~ curved, twisted, and tapered beam-like structure and local frame (left), taper and twist functions (right)

The position of the points in the current state are defined in a similar manner by means of the (current) mapping function

$$R_A(z_i,t) = R_{0A}(z_1,t) + x_\alpha(z_i) a_\alpha(z_1,t) + w_k(z_i,t) a_k(z_1,t) \tag{12}$$

where R_{0A} is a function mapping the position of the ~~points of the~~ centre-line points in the current state, while w_k are the components of the 3D warping displacements in ~~the~~ local frame a_k. The main formal difference between the reference map and the current ~~maps~~one is due to the warping, w, introduced to describe the geometry of the deformed state without a-priori approximation.

By using ~~the~~ maps (9) and (12), we can determine the 3D tensor, H, expressing the gradient of the current position, R_A, with respect to the reference position, R_B, as follows (see, for example, Rubin 2000)

$$H = \frac{\partial R_A}{\partial R_B} = G_k \otimes g^k \tag{13}$$

In (13), G_k and g^k are covariant and controvariant base vectors, in the current and reference states, and can be calculated by using standard mathematical methods (see, for example, Rubin 2000). In this case they can be written in the form

$$\begin{aligned}
g^1 &= g_0^{-1/2} b_1 \\
g^2 &= \Lambda_{22}^{-1}(b_2 - K^*_{B2\alpha} z_\alpha g_0^{-1/2} b_1) \\
g^3 &= \Lambda_{33}^{-1}(b_3 - K^*_{B3\alpha} z_\alpha g_0^{-1/2} b_1) \\
G_1 &= a_1 + \gamma_i a_i + K^*_{Ai\alpha} z_\alpha a_i + K_{Aij} w_j a_i + w_{i,1} a_i \\
G_2 &= \Lambda_{22} a_2 + w_{i,2} a_i \\
G_3 &= \Lambda_{33} a_3 + w_{i,3} a_i
\end{aligned} \tag{14}$$

where

$$\begin{aligned}
g_0^{1/2} &= 1 + K^*_{B1\alpha} z_\alpha \\
K^*_{(B\,or\,A)i\alpha} &= \Lambda'_{i\alpha} + \Lambda_{\beta\alpha} K_{(B\,or\,A)i\beta}
\end{aligned} \tag{15}$$

When H is known, the 3D Green-Lagrange strain tensor, E, can be calculated (see, for example, Rubin 2000 and Gurtin 2003). Hereafter we write ~~the~~ tensor E in a form based on simplifying assumptions applicable to the considered beam-like structure. In particular, we introduce the characteristic dimension of the cross-sections, herein denoted as h, the longitudinal dimension of the centre-line, herein denoted as L, and we assume h to be much smaller than L. Moreover, we consider a thin structure and assume the curvatures of its reference centre-line are much smaller than 1/h (see also Rubin 2000). In addition, we assume the warping displacements, w_k, are small. More precisely, by introducing a non-dimensional parameter ε much smaller than one, they ~~are~~come to be considered of the order of hε, while the order of magnitude of their derivative with respect to z_1 is εh/L. In general, all deformation measures, i.e. the 1D strain measures γ and k and the components of the 3D strain tensor, E, are assumed to be small. In particular, their order of magnitude is at most ε. For the considered structure, in the case of small strains and small local rotations, we write the strain tensor, E, in the following form

$$E \simeq \frac{T^T H + H^T T}{2} - I \tag{16}$$

Let's now calculate the components of E by using (16) and neglecting terms smaller than ε. Algebraic manipulations, which are based on equations (13)-(16), ~~yields~~yield the following expressions for bi-tapered cross-sections

$$\begin{aligned} E_{11} &= \gamma_1 + k_2\Lambda_{33}z_3 - k_3\Lambda_{22}z_2 \\ E_{22} &= \Lambda_{22}^{-1}w_{2,2} \\ E_{33} &= \Lambda_{33}^{-1}w_{3,3} \\ 2E_{21} &= \gamma_2 + \Lambda_{22}^{-1}w_{1,2} - k_1\Lambda_{33}z_3 \\ 2E_{31} &= \gamma_3 + \Lambda_{33}^{-1}w_{1,3} + k_1\Lambda_{22}z_2 \\ 2E_{23} &= \Lambda_{33}^{-1}w_{2,3} + \Lambda_{22}^{-1}w_{2,2} \end{aligned} \tag{17}$$

In (17), Λ_{22} and Λ_{33} are the edge-wise and flap-wise taper coefficients (see, for example, Figure 2), while the components of the strain tensor, E, are taken with respect to the reference local frame, b_i, i.e.

$$E_{ij} = E \cdot b_i \otimes b_j \tag{18}$$

where $\cdot$ is the usual scalar (or dot) product and $\otimes$ is the tensor (or dyadic) product (see, for example, Rubin 2000).

3.2 Stress fields and constitutive models

Given the strain tensor, E, the stress fields in the structure can be calculated when a constitutive model is chosen. Limiting our attention to elastic bodies, in a ~~pure~~purely mechanical theory, in the case of small strain, we use the following linear relation between the second Piola-Kirchhoff stress tensor, S, and the Green-Lagrange strain tensor (see, for example, Gurtin 2003)

$$S = 2\mu\, E + \lambda tr E\, I \tag{19}$$

where μ and λ are known material parameters related to ~~the~~ Young's modulus and Poisson's ratio. In the case of small strains and small local rotations, we also write

$$P \simeq TS, \quad C \simeq TST^T \tag{20}$$

where P is the first Piola-Kirchhoff stress tensor and C is the Cauchy stress tensor (Gurtin 2003). It is worth noting that in the considered case the tensor field T is sufficient to determine two of the above mentioned stress tensors (e.g. P and C) when the other one (e.g. S) is known.

We are now in ~~the~~a position to define the cross-sectional stress resultants, namely the force F and moment M. Using the first Piola-Kirchhoff stress tensor (Gurtin 2003), in the case of small warpings, small strains and small local rotations, we write

$$F = T\int_\Sigma P_{i1}b_i, \quad M = T\int_\Sigma x_\alpha P_{i1}\, b_\alpha \wedge b_i \tag{21}$$

where Σ is the domain corresponding to the cross-section on which the integration is performed and

$$P_{ij} = P \cdot a_i \otimes b_j \tag{22}$$

By combining equations (16)-(21), the force and moment stress resultants can be related to the geometrical parameters of the structure and the 1D strain measures (8). However, such relations are actually known only if we know the warping fields w_k. ~~An~~One approach to ~~obtain~~obtaining suitable warping fields is illustrated in section 3.4.

3.3 Expended power and balance equations

To complete the formulation, we conclude with considerations on the principle of expended power and the balance equations for the considered structure. For hyper-elastic bodies (Gurtin 2003), we write the principle of expended power in the form

$$\int_A p \cdot v + \int_V b \cdot v = \frac{d}{dt}\int_V \Phi \tag{23}$$

In (23), p are surface loads per unit reference surface (A), b are body loads per unit reference volume (V), Φ is the 3D energy density function of the body, which is half the scalar product of the tensor fields S and E (i.e. $2\Phi = S \cdot E$), and, finally, v is the time rate of change of the current position of the body's points, which is given by

$$v = v_0 + \omega \wedge x_\alpha a_\alpha + \dot{w} \tag{24}$$

where the last term in (24) is the time rate of change of the warping displacement.

For small warpings, small strains, and small local rotations, if the power expended by surface and body loads on the warping velocities is neglected, the external power, Π_e, reduces to the following form

$$\Pi_e = \Delta\left(F \cdot v_0 + M \cdot \omega\right) + \int_s F_s \cdot v_0 + M_s \cdot \omega \tag{25}$$

where the vector field v_0 is the time rate of change of the position of the ~~points of the~~ current centre-line points, the vector field ω is the time rate of change of the orientation of ~~the~~ vectors a_i, the terms F_s and M_s are suitable resultants of inertial actions and prescribed loads per unit length in the reference state, while the symbol Δ simply ~~means~~indicates that the function between brackets is evaluated at both the ends of the beam and the difference between those values is taken.

The cross-sectional warpings may be important in calculating the 3D energy function and cannot be neglected in the internal power, Π_i. However, the internal power may be reduced to a useful form for beam-like structures by introducing a suitable 1D strain energy function, U. For example, if U can be expressed in terms of the strain measures, γ and k, we can write

$$\Pi_i = \frac{d}{dt}\int_s U(\gamma, k, s) = \int_s f \cdot \dot{\gamma} + m \cdot \dot{k} \tag{26}$$

where the vector fields f and m are defined in terms of the force and moment stress resultants, F and M, as follows

$$f = T^T F, \quad m = T^T M \tag{27}$$

By using the principle of expended power, we also obtain balance equations for the vector fields F and M in the form

$$\begin{aligned} F' + F_s &= 0 \\ M' + R'_{0A} \wedge F + M_s &= 0 \end{aligned} \tag{28}$$

At this point, we have kinematic equations, (6)-(7), strain measures, (8) and (16), force and moment balance equations, (28), and the principle of expended power, $\Pi_e=\Pi_i$, in a suitable form for beam-like structures, (25)-(26). To complete the formulation of the model we need relations providing the 1D stress resultants in terms of the 1D strain measures. To this end, we need to know the warping fields. An approach to ~~obtain~~obtaining suitable warping functions is discussed ~~hereafter~~in the next section.

3.4 Warping displacements

In general, a 3D nonlinear elasticity problem can be formulated as a variational problem. ~~In any case~~However, if we try to solve the variational problem directly, the difficulties encountered in solving the elasticity problem remain. For beam-like structures whose transversal dimensions are much smaller than the longitudinal one, assumptions based on the shape of the structure and the smallness of the warping and strain fields can lead to useful simplifications. In particular, ~~the resolution of~~solving the 3D nonlinear elasticity problem can be reduced to ~~the resolution~~solution of two main problems. See, for example, Berdichevsky (1981), who seems to be the first in the literature to plainly state ~~that~~this for elastic rods. One of ~~those~~the two problems governs the local distortion of the cross-sections and is ~~here~~ referred to here as the cross-sections problem. The other ~~problem~~ governs the global deformation of the centre-line and is ~~here~~ referred to here as the centre-line problem. Hereafter, we consider the following variational statement to determine the warping fields which are responsible ~~of the~~for deformation of the cross-sections

$$\delta\int_V \Phi = 0 \tag{29}$$

In (29) the symbol δ stands for the variation operator and the density function Φ depends on the warping displacements. The warping fields satisfying (29) can be obtained by the corresponding Euler-Lagrange equations (see, for example, Courant 1953), by using numerical methods, in general, or analytical approaches providing closed-form expressions, in some particular cases. Once such a problem is solved, the components of the stress resultants (21) can be linearly related to the components of the 1D strain measures, by using equations (16)-(21). Then, if it is preferred or deemed useful, ~~those~~the resulting relations can also be arranged in ~~a~~ standard matrix form.

Note that to determine the current state of the structure we also need the displacements of its centre-line points. They can be determined by solving the centre-line problem, which is a non-linear problem governed by the set of kinematic, constitutive and balance equations introduced in section 3 (in particular, we are referring to the constitutive model in section 3.2, which relates stress resultants and strain measures, and the balance equations for the stress resultants in section 3.3).

In the next sections we show some analytical solutions (section 4) and numerical results (section 5) that can be obtained by applying the proposed modelling approach to some reference beam-like structures.

4 First analytical results for bi-tapered cross-sections

In this section we consider the case of a beam-like structure with bi-tapered elliptical cross-sections. For this case we can ~~provide~~obtain analytical solutions in terms of warping fields, while for generic shapes (e.g. the aerodynamic profiles used in wind ~~turbine blades,~~ and steam turbines blades, ~~and~~ as well as helicopter rotor blades ~~as well~~) the problem corresponding to (29) can be solved ~~by~~ using numerical methods. However, this is not surprising, since ~~even in the classical linear theory of prismatic beams~~ analytical solutions are available only for a limited number of cases ~~only~~even in the classical linear theory of prismatic beams (see, for example, Love 1944).

As discussed in section 3, we are assuming ~~the smallness of~~that the warpings, strains and local rotations are small. Moreover, hereafter we choose that the current local frames ~~to~~ be tangent to the current centre-line and ~~we~~ include possible shear deformations within the warping fields. In addition, with the aim of showing a first analytical solution for bi-tapered cross-sections, ~~in this section~~here we neglect the effects of the initial ~~twist of the~~ cross-~~sections.~~sectional twist. Then, we write the Euler-Lagrange equations corresponding to (29), whose unknown functions are the warping fields, w_k. ~~This~~ (this can be done ~~by~~ using standard mathematical techniques ~~(~~, see, for example, Courant 1953). Finally, we proceed to find a solution to the resulting (partial differential equations) problem. In particular, if we neglect the terms smaller than ε and maintain ~~the terms~~those related to extension, γ_1, and ~~change of curvatures~~changes in curvature, k_i, the ~~mentioned~~aforementioned Euler-Lagrange equations are satisfied by the following warping fields

$$\begin{aligned} w_1 &= k_1 \frac{\rho^2 d_3^2 - d_2^2}{\rho^2 d_3^2 + d_2^2} \rho \Lambda^2 z_2 z_3 \\ w_2 &= -\nu\gamma_1 \Lambda z_2 - \nu k_2 \rho \Lambda^2 z_2 z_3 + \nu k_3 \Lambda^2 (\rho^2 z_3^2 - z_2^2)/2 \\ w_3 &= -\nu\gamma_1 \rho \Lambda z_3 + \nu k_3 \rho \Lambda^2 z_2 z_3 - \nu k_2 \Lambda^2 (\rho^2 z_3^2 - z_2^2)/2 \end{aligned} \tag{30}$$

where d_2 and d_3 are the major semi-axes of a reference elliptical cross-section (e.g. the one at 18m from the root section in Figure 2), while $\Lambda=\Lambda_{22}$ and $\rho=\Lambda_{33}/\Lambda_{22}$ are known functions of z_1. Using this result, we can calculate the corresponding strain and stress fields, (16)-(20), stress resultants, (21), and strain energy function U. For example, if we consider a local frame in the reference cross-section with its origin at the cross-section's centre of mass and its axes aligned with the cross-section's principal axes of inertia (as in Figure 2), we can write the 1D strain energy function, U, in the form

$$U = \frac{1}{2} EA\rho\Lambda^2 \gamma_1^2 + \frac{1}{2} GJ_1 \rho^2 \Lambda^4 k_1^2 + \frac{1}{2} EJ_2 \rho^3 \Lambda^4 k_2^2 + \frac{1}{2} EJ_3 \rho \Lambda^4 k_3^2 \tag{31}$$

In (31), E is the Young modulus, G is the shear modulus, while A, J_1, J_2 and J_3 are the following geometrical parameters

$$A = \pi d_2 d_3, \;\; J_1 = A d_2^2 d_3^2 / (\rho d_3^2 + \rho^{-1} d_2^2), \;\; J_2 = A d_3^2 / 4, \;\; J_3 = A d_2^2 / 4 \tag{32}$$

An interesting result is that the initial taper appears explicitly in all the previous relations (in terms of ρ and Λ). ~~In its~~This, in turn, ~~this~~ allows ~~an~~ analytical evaluation of its effects on the 3D strain fields, which can be calculated by using (17) and (30~~),~~) and ~~which~~ are, in any case, required to determine the 3D stress fields (19).

5 Numerical simulations

In this section we ~~provide~~present the results of simulations conducted ~~by~~ using the modelling approach discussed in section 3, which we have implemented into a numerical code in MATLAB language. ~~Those~~The results are also compared with ~~the results that can be obtained by~~those obtainable via 3D-FEM simulations with the commercial software ANSYS.

In particular, we show a first set of test cases in which a beam-like structure with rectangular cross-sections undergoes large displacements, while ~~it is~~ fixed at one end and ~~it is~~ loaded at the other ~~end~~ by a force ~~whose magnitude is~~ of progressively ~~increased. In the~~increasing magnitude. The second set of test cases ~~we consider~~addresses a more complex geometry, that is, a beam-like structure with elliptical cross-sections, which is curved, twisted and tapered in its reference configuration, ~~while~~under the same loading condition ~~is the same~~ as in the first set of test cases. Finally, ~~in~~ the third set of test cases~~, we consider (~~ regards four~~)~~ different beam-like structures under the same loading ~~condition.~~conditions. In particular, we consider a first prismatic structure with elliptical cross-sections. The second structure is a modification of the first ~~one~~, on which ~~we maintain~~ the same cross-section is maintained at 18m from the root ~~and we add the~~ , while taper is added according to the taper coefficients ~~of~~in Figure 2. Starting ~~from~~ with this latter, we then consider a third structure which includes ~~the twist~~twisting of the cross-sections, assuming the twist law ~~of~~in Figure 2. The fourth ~~one~~and final case is a curved, twisted and tapered structure obtained ~~by~~from the third ~~one~~ (tapered and twisted) by adding ~~the~~a centre-line curvature. ~~Then~~Once the simulations have been completed, we compare the results obtained ~~by simulating the behaviour of these four structures~~ to ~~shows~~highlight the effects ~~related to~~ of their ~~geometrical differences~~different geometries on their mechanical behaviour.

In all ~~the~~ cases, the displacements of the ~~points of the~~ reference centre-line points are calculated by solving the centre-line nonlinear problem through ~~a~~the previously mentioned numerical procedure we have implemented in MATLAB ~~language~~, which is based on the kinematic, constitutive and balance equations introduced in section 3. In particular, ~~we use~~ the constitutive model introduced in section 3.2 is used to relate stress resultants and strain measures. We define the local frames orientation ~~by~~ using Euler angles and simulate orientation changes in terms of the derivatives of those angles over the arch-length, s (see, for example, Pai 2003). We use the balance equations for the stress resultants introduced in section 3.3. Finally, ~~we integrate (numerically)~~ the resulting set of ordinary differential equations is (numerically) integrated with respect to the reference arch-length, s. The results of this procedure are illustrated ~~hereafter~~in the following sections.

5.1 First set of test cases

In this set of test cases we consider a rectangular cross-sectioned beam-like structure ~~with rectangular cross-sections undergoing~~which undergoes large displacements, while ~~it is~~ clamped at one end (i.e. the root) and ~~it is~~ loaded at the other ~~end~~ (i.e. the tip) by a force, F, whose magnitude is progressively increased (see Figure 3). The centre-line length is d_1=90m~~.~~ ~~The~~, while the cross-section ~~sizes~~dimensions are d_2=8m (edge-wise) and d_3=2m (flap-wise). The material properties are

summarized by reference values of ~~the~~ Young's modulus, 70GPa, and Poisson's ratio, 0.25. ~~The~~Finally, the flap-wise tip force, F, varies from 100kN to 75000kN.

The simulations are run for different values of the tip force. The model we have implemented in MATLAB ~~language to solve~~for solving the non-linear problem ~~provides~~renders results on the structure's deformed configuration ~~of the structure~~ (e.g. Figure 3, left) within a few seconds. In all ~~the~~ cases, the simulation time is less than 2.4s~~. It~~, which is significantly less than that required ~~by~~for the corresponding non-linear 3D-FEM simulations carried out on the same computer, while the accuracy of the results is almost the same. A summary of the results obtained ~~results~~, in terms of global displacements and simulation times, is shown in Figures 3 and 4.

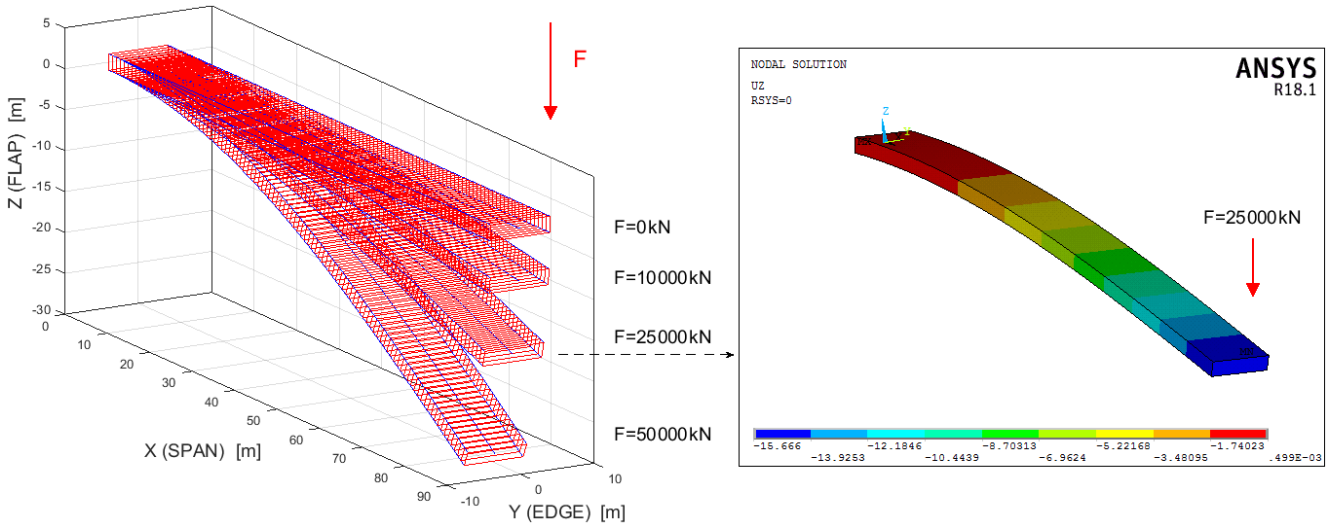

Figure 3: Global deformation with 3D-BLM for ~~F~~ increasing F (left) and with 3D-FEM for F=25000kN (right)

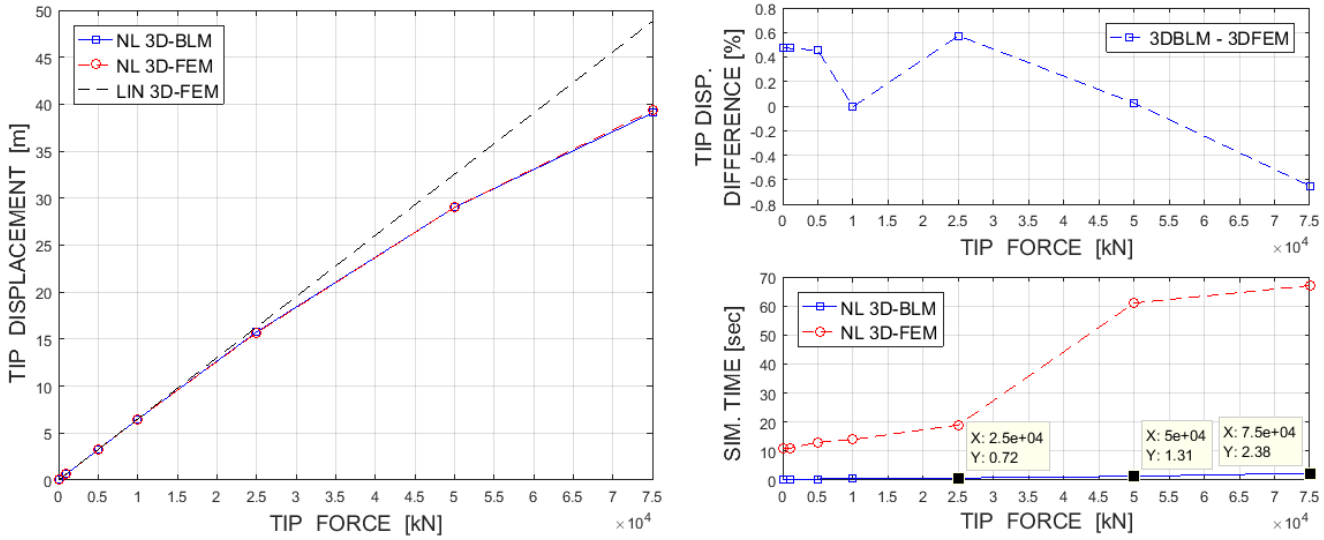

Figure 4: Comparison of tip displacements (left), tip ~~displacements~~displacement differences and simulation times (right)

In particular, Figure 3 (left) shows the un-deformed shape (for F=0), as well as the deformed shapes for F equal to 10000kN, 25000kN and 50000kN. Figure 3 (right) shows the 3D-FEM deformed shape for F=25000kN (the coloured ~~legend~~scale is for the flap-wise displacements). ~~Then,~~ Figure 4 (left) provides a comparison between the tip displacements obtained with the linear 3D-FEM, the nonlinear 3D-FEM and our model (~~therein referred to~~indicated as 3D-BLM). It also shows the differences (between the non-linear 3D-FEM and the 3D-BLM) in terms of tip displacements and simulation times for the considered cases.

5.2 Second set of test cases

Let's now consider a more complex beam-like structure, ~~more precisely,~~specifically, one with a 90m curved centre-line with constant curvatures, which schematizes a pre-bent and swept beam whose tip is moved 4m edgewise and 3m flap-wise, as in Figure 2. The local frames in the reference state are characterized by a pre-twist of 20deg/m. The reference cross-section at 18m from the root is an ellipse whose major semi-axes are d_2=2m (edge-wise) and d_3=0.5m (flap-wise). The sizes of the other cross-sections change according to the taper coefficients ~~of~~in Figure 2. ~~For what the~~The material properties are ~~concerned, they are summarized~~represented by reference values of ~~the~~ Young's modulus, 70GPa, and Poisson's ratio, 0.25. Finally, the structure is clamped at its root and ~~it is~~ loaded by a flap-wise tip force, F, which varies from 100kN to 1000kN.

The simulations are run for different values of tip force, F. The model we have implemented in MATLAB ~~language to solve~~for solving the non-linear problem ~~provides~~yields results ~~about~~regarding the structure's deformed configurations ~~of the structure~~, such as those in Figure 5, which confirm the computational efficiency and accuracy observed in the previous ~~section.~~tests. In particular, ~~the~~ simulation ~~time is~~times are significantly ~~less~~shorter than ~~that~~those required by corresponding

nonlinear 3D-FEM simulations (see, for example, the simulation times' ratio in Figure 6, right), while the accuracy of the results is again ~~almost~~nearly the same (Figure 6).

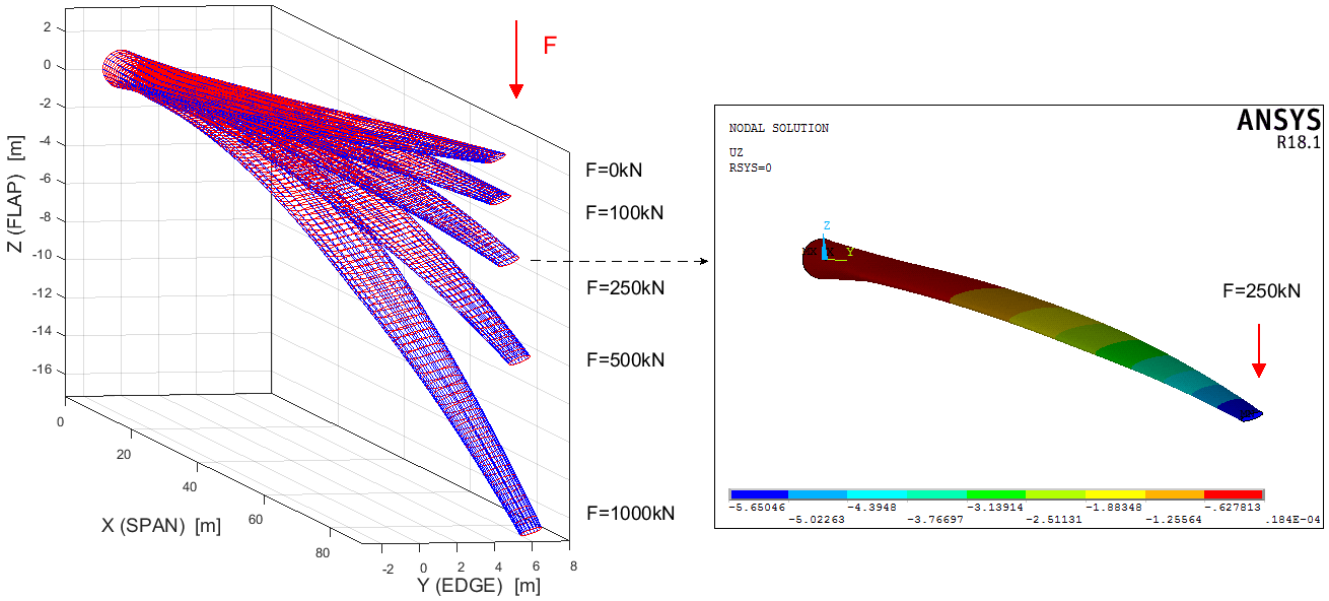

Figure 5: Global deformation with 3D-BLM for ~~F~~ increasing F (left) and with 3D-FEM for F=250kN (right)

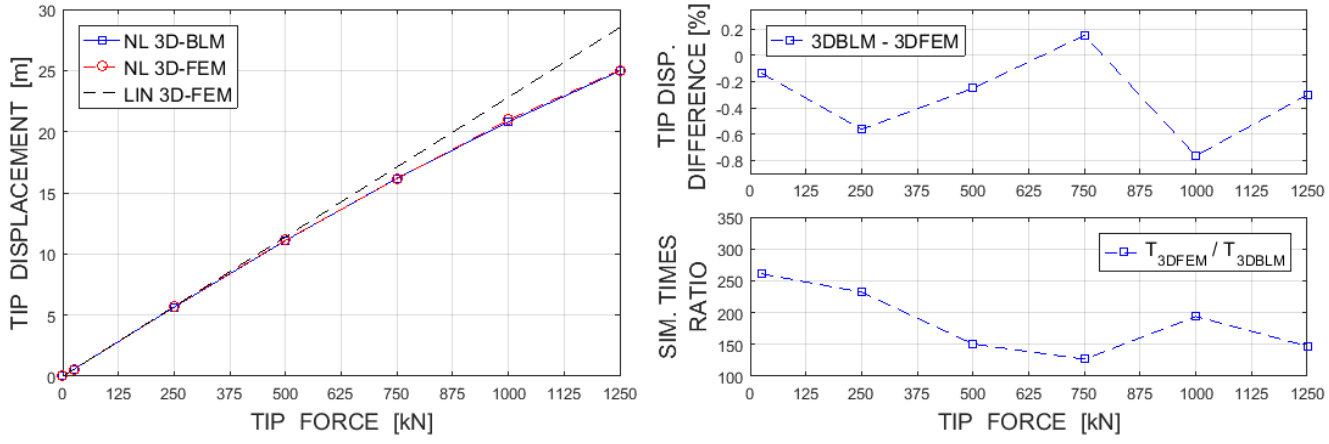

Figure 6: Comparison of tip displacements (left), tip ~~displacements~~ displacement differences and simulation times ratio (right)

~~Hereafter, we continue by showing~~Apart from the foregoing results, the model is also able to provide other meaningful information ~~our model can provide.~~. In particular, we can obtain the displacement fields of the ~~points of the~~ reference centre-line points (Figure 7), as well as the change ~~of curvatures~~in curvature of the beam-like structure (Figure 8, left) and the corresponding moment stress resultant (Figure 8, right). The moment components are in the current local frame, a_i, whose

orientation has been determined as part of the solution ~~of~~to the nonlinear problem. For example, the orientation of the current local frame, a_i, can be ~~provided~~expressed in terms of a set of Euler angles, as in Figure 9. In this case we have considered the set of Euler angles corresponding to a first rotation, θ, about the initial z-axis, a second rotation, γ, about the intermediate y-axis, and a third rotation, ψ, about the final x-axis.

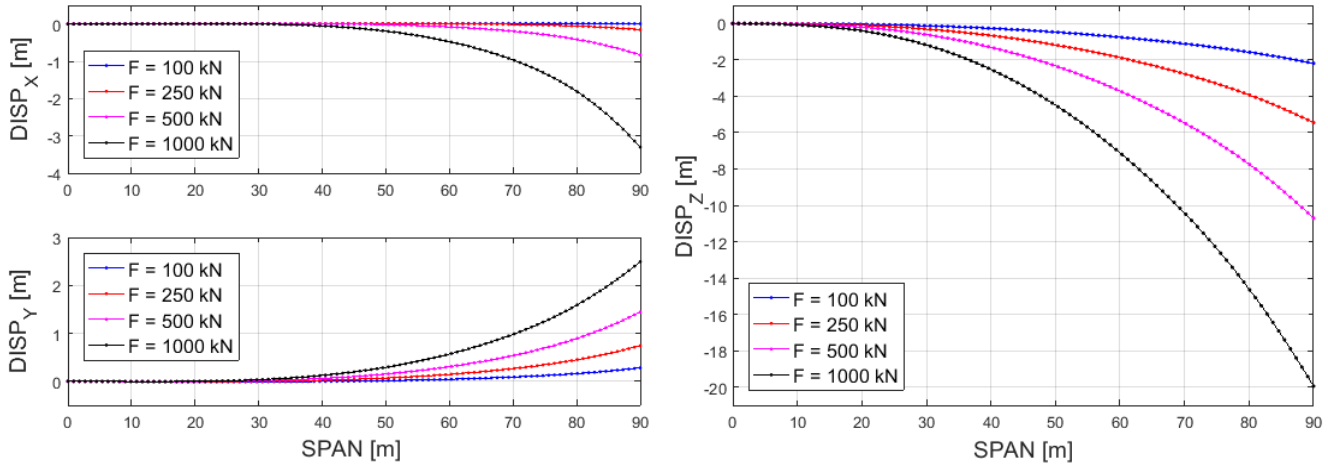

Figure 7: Displacement of the ~~points of the~~ reference centre-line points with 3D-BLM for ~~F~~ increasing F

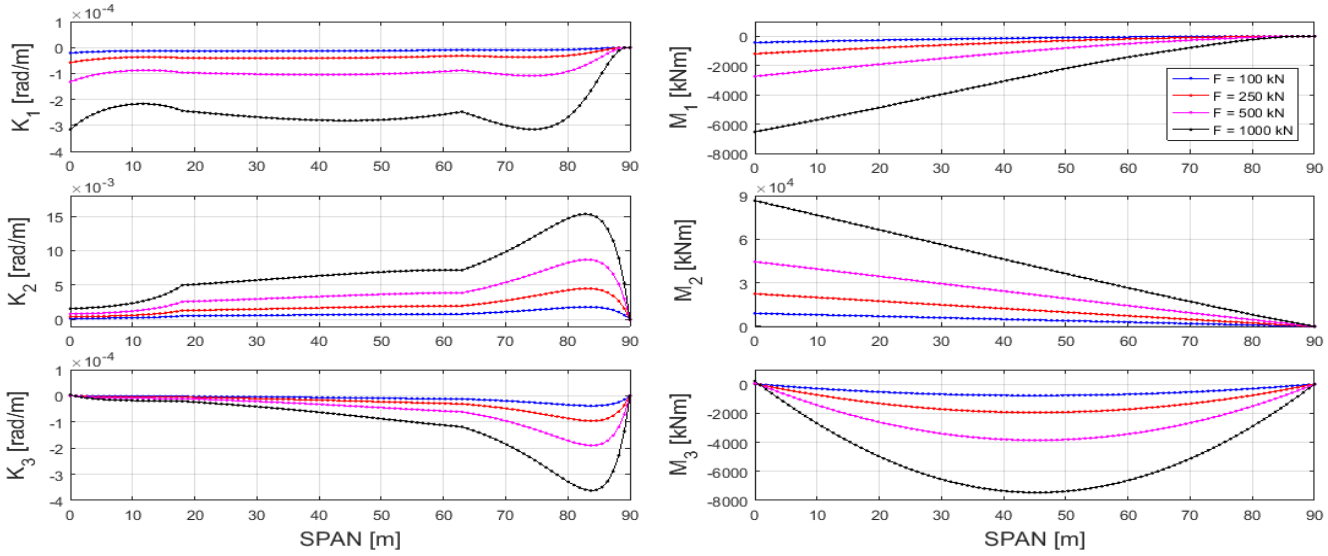

Figure 8: Changes ~~of curvatures~~in curvature (left) and moment stress resultants (right) with 3D-BLM for ~~F~~ increasing F

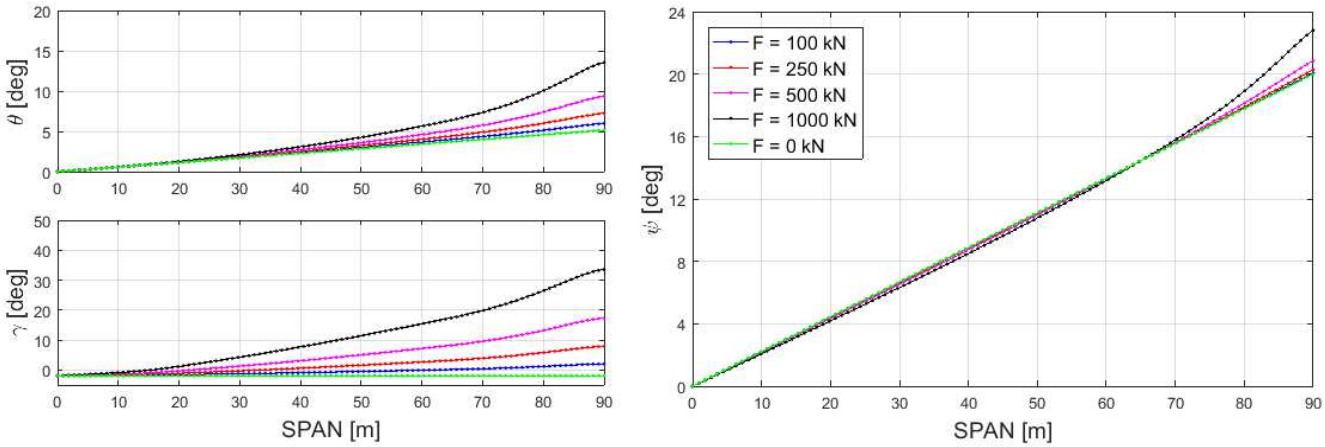

Figure 9: Local frames orientation in terms of Euler angles before (green-lines) and after deformation

5.3 Third set of test cases

~~Here we consider~~The last test cases regard four different beam-like structures, starting with a prismatic elliptical one, ~~including~~ to which there is the step~~-~~by~~-~~step addition of the taper~~ and,~~ the twist of the cross-sections and, finally, the curvature of the centre-line, as discussed in~~ the beginning of~~ section 5. Note that the "curved-twisted-tapered" case considered here coincides with that discussed ~~with~~in more ~~details~~detail in section 5.2 (see Figures 5-9, F=250kN). We begin by simulating the behaviour of these four structures under a flap-wise tip force of 250kN. Then, we analyze the results obtained ~~results~~ to show the effect of ~~their~~the geometric differences on their mechanical behaviour.~~ A summary of the~~ The results obtained ~~results is hereafter.~~are summarized in the following. In particular, Figure 10 shows the reference and deformed states of the prismatic structure (left) and the deformed states of the non-prismatic ones (right), while Figure 11 shows the displacements of their centre-~~lines~~line points. The main effect of the considered tip force is a displacement in the z-direction~~,~~ in all ~~the~~ cases, with a displacement in the y-direction ~~that we have only~~ for the ~~cases~~ "tapered-twisted" and "tapered-twisted-curved~~",~~" cases only, as it ~~is~~would be expected.

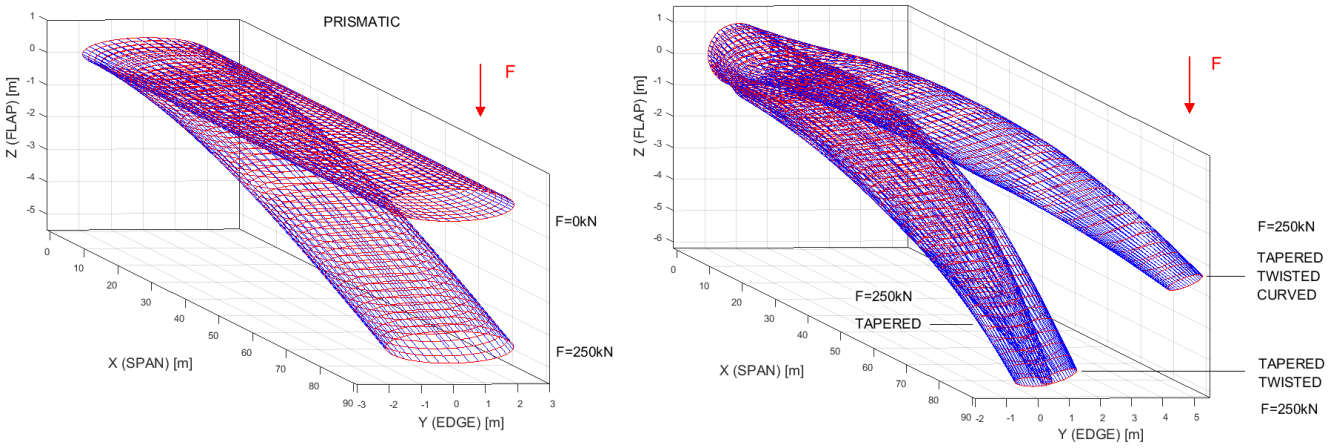

Figure 10: Prismatic case before and after deformation (left) and non-prismatic cases after deformation (right)

425

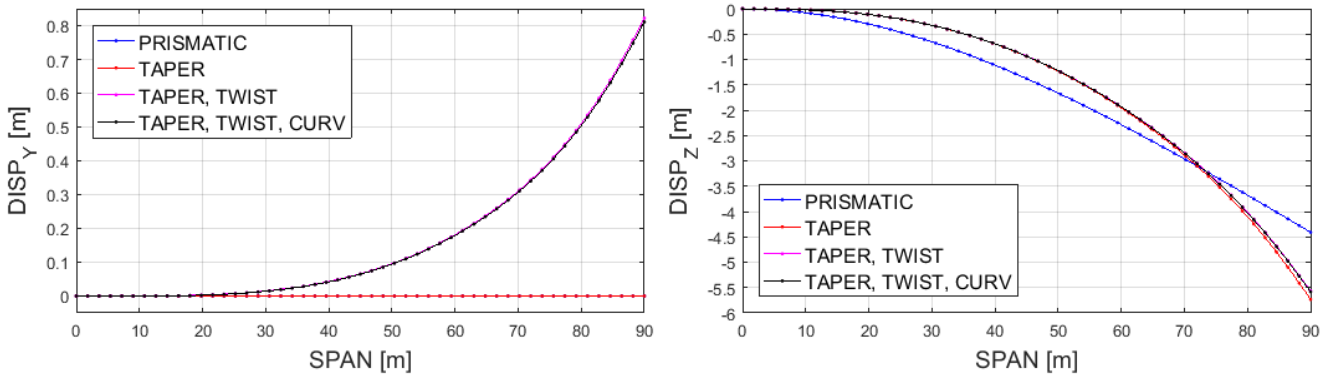

Figure 11: ~~Displacement of centre~~Centre-line points displacement of prismatic case (blue) and non-prismatic cases (other colours) for F=250kN

430 Similar results have also been obtained ~~also~~ for larger values of tip-force, F, which lead to larger tip-displacements. In particular, ~~such a force,~~ hereafter we show the results for F~~, is varied~~ varying from 250kN to 750kN. As for the previous test cases, the results obtained ~~results~~ have been compared with those ~~of~~from 3D-FEM simulations, confirming the computational efficiency and accuracy ~~pointed out~~revealed in the previous sections. A ~~results'~~ summary is shown in Figure 12, which provides a comparison in terms of tip-displacements, for the four geometries considered here, for F=250kN, 435 F=500kN and F=750kN. Such loads correspond, respectively, to tip-displacements of about 6.4%, 12.5% and 18.1% of the span-wise reference length. The difference between the 3D-BLM and the non-linear 3D-FEM in terms of tip-displacements is ~~always~~ below 0.9% in all the considered cases (Figure 12).

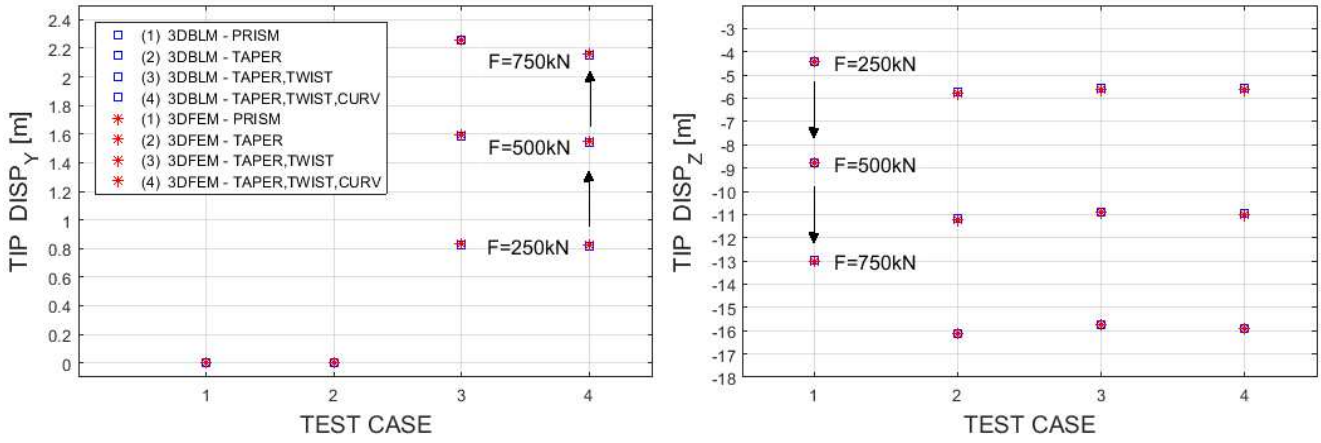

Figure 12: Tip displacements with 3D-BLM (blue) and 3D-FEM (red) for different geometries and ~~F~~ increasing F (see arrows)

~~Hereafter, we~~We conclude ~~with comparison~~now by examining the results for the 3D strain measure E_{11}, also referred to as longitudinal strain, which is another important parameter for the ~~analyses~~analysis and design of rotor blades (see, for example, Griffith 2011). In particular, we focus ~~the attention~~ on the effects of taper by considering a beam-like structure with bi-tapered cross-sections (the above "test case 2"). Then, we compare the outcomes of the 3D-BLM with those of linear and nonlinear 3D-FEM simulations. A ~~results'~~ summary of the results is reported in Figure 13~~. It~~, which shows the maximum longitudinal strain at different reference cross-sections (~~those ones~~ at 30%, 50%, and 70% of the span-wise reference length) and for three different tip~~-~~ forces (F=250kN, F=500kN and F=750N).

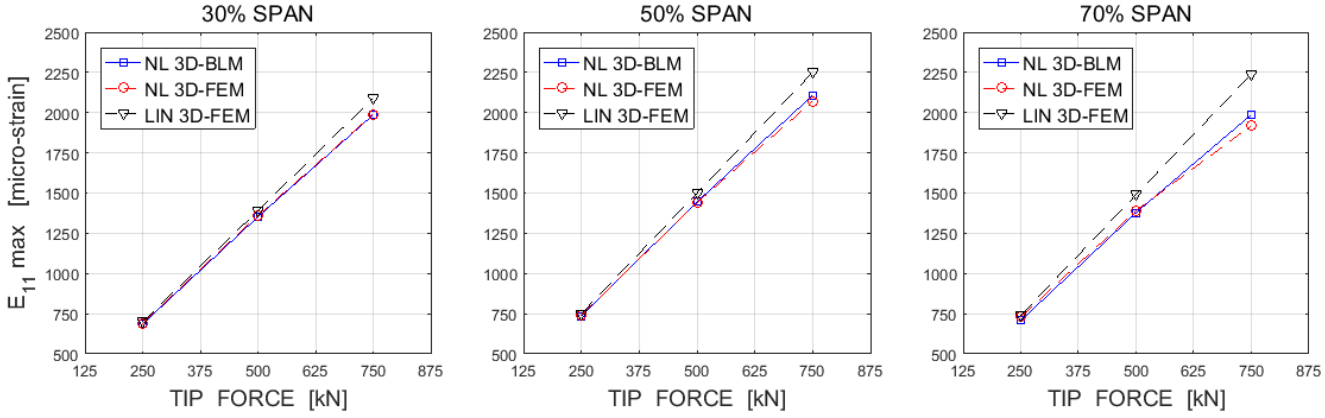

Figure 13: Max longitudinal strain E_{11} in ~~the~~ cross-sections at 30%, 50% and 70% span for ~~F~~ increasing F (bi-tapered case)

As verified by many simulations and shown in the examples, the proposed approach performs well in terms of computational efficiency and accuracy. It can be used to study the mechanical behaviour of beam-like structures, which are curved, twisted and tapered in their ~~reference~~ unstressed reference state and undergo large global displacements. It can moreover provide

information on the deformed configurations of ~~those~~the structures, such as their displacement fields, as well as the corresponding strain and stress measures. It is worth noting that it is suitable for beam-like structures with generic reference cross-sections shapes. However, as already pointed out, for bi-tapered elliptical cross-sections ~~we have~~ analytical solutions can be obtained in terms of warping fields, while for generic reference cross-sections shapes ~~the~~ problem (29) has to be solved ~~by~~ using numerical methods.

6 Conclusions

~~Wind turbine blades, as well as helicopter rotor blades, steam turbine blades and many other~~ Many complex engineering structures, ~~can be considered complex (~~such as the rotor blades of wind turbines and helicopters, are non-prismatic~~)~~ beam-like structures, with one dimension much larger than the other two and a shape that is curved, twisted and also tapered ~~already~~ in the ~~reference~~ unstressed reference state. ~~Their mechanical~~ The increasing size and flexibility of such structures make the prediction of their aero-elastic behaviour ~~can be simulated through suitable 3D beam models, which are~~ever more challenging. This paper addressed the structural part of this modelling and proposed a modelling approach, referred to as 3D-BLM, which is computationally efficient, accurate and explicitly consider the main geometrical ~~design features~~characteristics of ~~those~~ the mentioned structures, the large deflections of their reference centre-line~~,~~ and the in- and out-of-plane warping of their transversal cross-sections. In ~~this work, curved, twisted and tapered beam like structures~~the mentioned approach, the warping displacements have been ~~modelled analytically. Their main geometrical characteristics have been explicitly included in the model. The warping displacement has been~~ thought of as an additional small motion superimposed ~~to~~on the global motion of the local frames. The ~~resulting model is suitable to simulate large deflections of the centre line, large rotations of the local frames and small deformation of the cross sections. The~~ strain tensor has been calculated analytically in terms of ~~the~~ geometrical parameters of the ~~considered structures, the~~structure, 1D strain measures and ~~the~~ 3D warping fields. ~~An approach~~A method based on ~~an energy functional and~~ a variational statement ~~have~~has been used to obtain suitable warping fields. The ~~principle of expended power for curved, twisted and tapered beam like structures has been discussed, along with the balance equations for the force and moment stress resultants. Finally,~~ proposed approach enables to obtain analytical results ~~and~~ in particular cases and can be implemented into an efficient numerical code in the general case. The analytical results obtained, along with numerical examples~~, which include comparison~~ (obtained by implementing 3D-BLM into a computer code) and comparisons with ~~3D~~ corresponding results from 3D-FEM simulations~~,~~ have been presented to show the effectiveness of the ~~proposed~~ modelling approach and the information it can provide. In all cases, the simulation times with 3D-BLM have been significantly shorter than those required by 3D-FEM simulations, while the accuracy of the results has been always almost the same. In this paper the analyses have been limited to the terms of order ε, as discussed in the introduction of the strain measures of the model. This turned out to be sufficient to accurately predict the global deflection of the considered structures even when the displacements of the centre-line points are large and nonlinear with respect to the applied loads. The inclusion of higher order terms in the model may provide better results,

especially in terms of stress and strain fields predictions, while not practically affecting the computational performance of the implemented model. This is an important point to be further investigated and will be the objective of a successive work. An interesting future activity would also be to performing comparison analyses with other structural modelling methods (not only 3D-FEM), with the aim of assessing the performance of different structural models for non-prismatic beam-like structures in terms of information each approach can provide (e.g. centre-line displacements, 1D strain measures, 3D strain fields), computational efficiency and results accuracy.

References

Antman S.S., Warner W.H., Dynamical theory of hyper-elastic rods, Arch. Rational Mech. Anal., 23, 135-162, 1966.

Ashwill T.D., Kanaby G., et al, Development of the swept twist adaptive rotor (STAR) blade, 48th AIAA Aerospace sciences meeting, Orlando, FL, Jan. 4-7, 2010.

Bak C., Zahle F., et al., Description of the DTU 10MW reference wind turbine, DTU Wind Energy Report-I-0092, Denmark, 2013.

Berdichevsky V.L., On the energy of an elastic rod, Journal of Applied Mathematics and Mechanics, 45, 518-529, 1981.

Bottasso C.L., Campagnolo F., et al, Optimization-based study of bend-twist coupled rotor blades for passive and integrated passive/active load alleviation, Wind Energy, 16, 1149-1166, 2012.

Courant R., Hilbert D., Methods of mathematical physics, Interscience Publisher, 1st ed., 1953.

Giavotto V., Borri M., et al, Anisotropic beam theory and applications, Computers and structures, 16, 1-4, 403-413, 1983.

Griffith D.T., Ashwill T.D., The Sandia 100-meter All-glass Baseline Wind Turbine Blade: SNL100-00, Sandia National Laboratories Report 3779, California, 2011.

Gurtin M.E., An introduction to continuum mechanics, Mathematics in science and engineering, Academic Press, 1st ed., 1981.

Hansen M.O.L., Sørensen J.N., et al, State of the art in wind turbine aerodynamics and aeroelasticity, Progress in Aerospace Engineering, 42, 285-330, 2006.

Hodges D.H., Review of composite rotor blades modeling, AIAA Journal, 28, 561-565, 1990.

Hodges D.H., Geometrically exact equations for beams, Encyclopedia of Continuum Mechanics, Springer Verlag, 2018.

Ibrahimbegovic A., On finite element implementation of geometrically nonlinear Reissner's beam theory: three-dimensional curved beam elements, Computer methods in applied mechanics and engineering, 122, 11-26, 1995.

Kunz D.L., Survey and comparison of engineering beam theories for helicopter rotor blades, Journal of Aircraft, 31, 473-479, 1994.

Leishman J.G., Principles of helicopter aerodynamics, Cambridge University Press, 2nd ed., 2016.

Love A.E.H., A treatise on the mathematical theory of elasticity, Dover Publications, 4th ed., 1944.

Pai P.F., Three kinematic representations for modeling of high flexible beams and their applications, Int. Journal of solids and structures, 48, 2764-2777, 2011.

Pai P.F., Problem in geometrically exact modeling of highly flexible beams, Thin-walled structures, 76, 65-76, 2014.

Rafiee M., Nitzsche F., Labrosse M., Dynamics, vibration and control of rotating composite beams and blades: a critical review, Thin-walled structures, 119, 795-819, 2017.

Reissner E., On finite deformation of space curved beams, Journal of applied mathematics and physics, 32, 734-744, 1981.

Rosen A., Friedmann P.P., Non linear equations of equilibrium for elastic helicopter or wind turbine blades undergoing moderate deformation, NASA, CR-159478, 1978.

Rosen A., Structural and dynamic behavior of pre-twisted rods and beams, American Society of Mechanical Engineers, 44, 483-515, 1991.

Rubin M.B., Cosserat theories: shells, rods and points, Solid mechanics and its applications, Springer Netherlands, 1st ed., 2000.

Ruta G., Pignataro M., Rizzi N., A direct one-dimensional beam model for the flexural-torsional buckling of thin-walled beams, Journal of Mechanics of materials and structures, 1, 1479-1496, 2006.

Simo J.C., A finite strain beam formulation, the three-dimensional dynamic problem, part I, Computer methods in applied mechanics and engineering, 49, 55-70, 1985.

Stäblein A.R., Hansen M.H., and Verelst D.R.: Modal properties and stability of bend-twist coupled wind turbine blades, Wind Energy Science, 2, 343-360, 2017.

Tanuma T., Advances in steam turbines for modern power plants, Woodhead Publishing, 1st ed., 2016.

Wang L., Liu X., Kolios A., State of the art in the aeroelasticity of wind turbine blades: aeroelastic modelling, Renewable and sustainable energy review, 64, 195-210, 2016a.

Wang Q., Johnson N., et al. Partitioned nonlinear structural analysis of wind turbines using BeamDyn, Proc. of the 34th ASME Wind Energy Symposium, San Diego, California, 2016b.

Wiser R., Jenni K., et al, Forecast wind energy costs and cost drivers: the views of the world's leading experts, LBNL 1005717, 2016.

Yu W., Hodges D.H., Ho J.C., Variational asymptotic beam-sectional analysis - an updated version, Int. Journal of engineering science, 59, 40-64, 2012.